[redacted]

RM No. E7K24

NACA

RESEARCH MEMORANDUM

for the

Bureau of Aeronautics, Navy Department

EFFICIENCY OF RADIAL-FLOW TURBINE OF TURBO ENGINEERING CORPORATION TT13-18 TURBOSUPERCHARGER

By Earl E. Coulter, and William R. Galloway

Flight Propulsion Research Laboratory
Cleveland, Ohio

[redacted]

TECHNICAL EDITING WAIVED

NATIONAL ADVISORY COMMITTEE FOR AERONAUTICS

WASHINGTON

DECEMBER [illegible] 1947

[redacted]

NATIONAL ADVISORY COMMITTEE FOR AERONAUTICS

RESEARCH MEMORANDUM

for the

Bureau of Aeronautics, Navy Department

EFFICIENCY OF RADIAL-FLOW TURBINE OF TURBO ENGINEERING CORPORATION TT13-18 TURBOSUPERCHARGER

By Earl E. Coulter and
William R. Galloway

SUMMARY

An investigation of the radial-flow turbine of a Turbo Engineering Corporation TT13-18 turbosupercharger was made to evaluate the effects of inlet total pressure, inlet total temperature, and pressure ratio on the adiabatic efficiency. The results are presented by three efficiency parameters. Inasmuch as variation of efficiency with inlet total pressure and temperature may be a Reynolds number effect, the efficiency is shown as a function of a Reynolds number factor.

Maximum efficiency obtained, based on total-pressure ratio and corrected for bearing friction, was 0.82 at an inlet total pressure of 50 inches of mercury absolute, an inlet total temperature of 1600° R, a total-pressure ratio of 1.46, and a blade-jet speed ratio of 0.62.

INTRODUCTION

At the request of the Bureau of Aeronautics, Navy Department, an investigation of the turbine from the Turbo Engineering Corporation TT13-18 turbosupercharger has been conducted at the NACA Cleveland laboratory to determine the effects of total pressure, total temperature, and pressure ratio on efficiency. The performance of the turbine of the XTT13-12 turbosupercharger, which is very similar to the TT13-18 turbine, is reported in reference 1. Because of the method of attaching the XTT13-12 turbine wheel to the shaft, the speed was limited to 17,000 rpm. No cooling air was used; the inlet total temperature was therefore limited to 1400° R.

[redacted]

In the present investigation, the turbine speeds ranged from 3000 to 24,000 rpm; inlet total pressures, from 20 to 50 inches of mercury absolute; inlet total temperatures, from 1200° to 2160° R; and total-pressure ratios, from 1.45 to 4.0 (ratio of inlet total to outlet static pressure, 1.5 to 5.0). The cooling-air weight flow was held at 0.44 to 0.49 pound per second when possible.

APPARATUS AND INSTRUMENTATION

The radial-flow turbines of the TT13-18 and XTT13-12 turbosuperchargers are unique in flow path and design. The combustion gas enters the nozzle box through two tangential inlet ducts, flows radially inward through the nozzle ring into the turbine wheel, and then discharges axially from the turbine. Because the gas flows radially inward against centrifugal force, the turbine operates with considerable reaction. Full peripheral admission is provided by 18 equally spaced nozzles in the nozzle ring. The turbine wheel and its 17 blades are integrally machined of high-temperature-resisting steel. Turbine-wheel cooling is provided by passing air through drilled passages under the roots of the blades.

The turbine assembly for the TT13-18 turbosupercharger is the same as that described in reference 1 for the XTT13-12 turbosupercharger with the following exceptions: (1) The waste-gate nozzle ring was closed off by the manufacturer; (2) the vacuum chamber for preventing distortion of the front section of the nozzle box under simulated altitude conditions was supplied by the manufacturer and was of different design; (3) a stiffening sleeve was installed on the turbine shaft between the front and rear bearings to add rigidity normally supplied by the compressor impellers in the complete turbosupercharger assembly; (4) the oil passages to the front bearing were different; and (5) the turbine wheel was attached to the shaft by a different method. The experimental setup is shown in figure 1. The various turbine clearances and the values of the cold clearances before and after 86 operating hours are presented in figure 2.

The instrumentation and the accuracy are the same as described in reference 1. In addition, the bearing loss was determined by measuring the oil flow through the bearings with a calibrated thin-plate orifice, measuring the temperature rise between the oil-inlet and oil-outlet lines with iron-constantan thermocouples, and calculating the rate of heat rejection to the bearing oil.

OPERATING CONDITIONS AND PROCEDURE

Efficiency investigations were made over a range of inlet total pressures, inlet total temperatures, and ratios of inlet total to outlet static pressure. The following table shows the approximate operating conditions:

Inlet total pressure (in. Hg abs.)	Inlet total temperature (^{o}R)	Ratio of inlet total to outlet static pressure
30	1200	1.5, 2.0, 3.0, 4.0, 5.0
30	1400	1.5, 2.0, 3.0, 4.0, 5.0
20	1600	1.5, 2.0, 3.0, 4.0, 5.0
30		2.0, 3.0, 5.0
50		1.5, 2.0, 3.0
30	1800	2.0, 5.0
30	2000	1.5, 2.0, 3.0, 4.0
30	2160	1.5, 2.0, 3.0

At each condition, the turbine speed was varied from a minimum of 3000 to 6000 rpm to a maximum of 24,000 rpm. Running was necessarily discontinued at some speed less than 24,000 rpm for low-power conditions, at which the minimum dynamometer absorption including bearing power loss, windage, and power absorption due to residual magnetism became equal to the turbine output at the lower speed.

The cooling-air flow rate was held within 0.44 to 0.49 pound per second when possible. At conditions of low gas density and low pressure ratio, an inlet total pressure of 20 inches of mercury absolute, and ratios of inlet total to outlet static pressure of 1.5, 2.0, and 3.0, the normal cooling-air flow rate could not be maintained and was lowered to 0.29 to 0.32 pound per second.

SYMBOLS

The following symbols are used in this report:

A_o area swept by trailing edges of turbine blades, square feet

g acceleration due to gravity, 32.2 feet per second per second or pounds per slug

M_t mass flow of air plus fuel, slugs per second

N turbine speed, rpm

P_i total pressure at nozzle-box inlet, inches of mercury absolute

P_o total pressure at turbine outlet computed from static pressure and average axial component of outlet-velocity pressure, inches of mercury absolute

p_o static pressure at turbine outlet, inches of mercury absolute

R_b gas constant for combustion products, foot-pounds per pound °R

T_i total temperature at nozzle-box inlet, °R

T_o total temperature at turbine outlet defined as sum of outlet static temperature and temperature equivalent of average axial component of outlet velocity head, °R

t_o static temperature at turbine outlet, °R

U blade tip speed, feet per second

V theoretical jet speed, feet per second

V_a average axial component of turbine-outlet velocity, feet per second

W_t weight flow of air plus fuel, pounds per second

γ ratio of specific heats

δ ratio of turbine-inlet total pressure to NACA standard sea-level pressure (P_i/29.92 in. Hg absolute)

η_s turbine adiabatic efficiency defined as ratio of measured shaft power to theoretically available power based on inlet total pressure and temperature and outlet static pressure

η_w turbine adiabatic efficiency defined as ratio of measured shaft power plus bearing power loss to theoretically available power based on inlet total pressure and temperature and outlet static pressure

η_p turbine adiabatic efficiency defined as ratio of measured shaft power plus bearing power loss to difference between theoretically available power based on inlet total pressure and temperature and outlet static pressure and power remaining in outlet gas computed from average axial component of outlet gas velocity

θ ratio of turbine-inlet total temperature to NACA standard sea-level temperature (T_1/519° R)

ρ_o average mass density of combustion gas at turbine outlet, slugs per cubic foot

ρ_{Hg} mass density of mercury at 32° F, slugs per cubic foot

850

CALCULATIONS

The gas temperatures were much higher than ambient-air temperatures and an appreciable amount of fuel was burned, which resulted in combustion products with thermodynamic properties differing from those of pure air. The thermodynamic data of reference 2 was therefore used for the calculation of the theoretically available work, the theoretical jet speed V, the gas constant R_b, and the ratio of specific heats γ.

The methods of calculating the turbine adiabatic efficiencies η_s and η_W are evident from their definitions. The efficiency η_P is defined mathematically as

$$\eta_P = \frac{\eta_W \left(\frac{M_t V^2}{2}\right)}{\left(\frac{M_t V^2}{2}\right) - \left(\frac{M_t V_a{}^2}{2}\right)} = \frac{\eta_W}{1 - \left(\frac{V_a}{V}\right)^2} \tag{1}$$

The average axial component of the outlet velocity V_a is equal to the mass flow M_t divided by the average mass density ρ_o and the area swept by the trailing edges of the blades A_o

$$V_a = \frac{M_t}{\rho_o A_o} \tag{2}$$

The average mass density of the gas at the outlet is

$$\rho_o = \frac{70.73 p_o}{g R_b t_o} \tag{3}$$

where

$$t_o = T_o - \frac{V_a{}^2(\gamma-1)}{2 g R_b \gamma} \tag{4}$$

Substituting equations (3) and (4) in equation (2) forms a quadratic equation in terms of V_a that yields

$$V_a = \sqrt{\left(70.73 \frac{\gamma}{\gamma-1} \frac{A_o p_o}{M_t}\right)^2 + \left(2g \frac{\gamma}{\gamma-1} R_b T_o\right)} - \left(70.73 \frac{\gamma}{\gamma-1} \frac{A_o p_o}{M_t}\right) \quad (5)$$

Equation (5) would require a cumbersome trial-and-error solution because the values of V_a, γ, and T_o are dependent upon each other. The effects of windage, conduction, radiation, and swirl in the outlet gas on the value of T_o were therefore neglected and T_o was calculated from figure 7 of reference 2. A value of γ corresponding to the inlet total temperature was used. These two approximations should introduce an error of less than 1 percent of the true value of V_a.

The outlet total pressure P_o is defined as

$$P_o = p_o + \frac{\rho_o V_a^{\,2}}{24 g \rho_{Hg}} \quad (6)$$

RESULTS

The performance of the turbine is presented by means of three adiabatic efficiencies: the ratio of the measured shaft power to the theoretically available power computed from inlet total pressure and temperature and outlet static pressure η_s; the ratio of the measured shaft power plus bearing power loss to the theoretically available power computed from inlet total pressure and temperature and outlet static pressure η_w; and the ratio of the measured shaft power plus bearing power loss to the difference between the theoretically available power computed from inlet total pressure and temperature and outlet static pressure and the power remaining in the outlet gas computed from the average axial component of the outlet gas velocity η_P. The data for the efficiency investigation of the TT13-18 turbosupercharger turbine are presented in table I. Maximum efficiency obtained based on total-pressure ratio and corrected for bearing power loss η_P was 0.82 at an inlet total pressure of 50 inches of mercury absolute, an inlet total temperature of 1600° R, a total-pressure ratio of 1.46, and a blade-jet speed ratio of 0.62.

The relative magnitude of the three adiabatic efficiencies is shown in figure 3. The blade-jet speed ratio at the maximum value of η_s is 0.59 and of η_w, 0.62. This shift in the blade-jet speed ratio at peak efficiency is caused by the rapid increase in bearing power loss with turbine speed shown in figure 4. No measurable change could be detected over a range of loads on the thrust bearing. For the maximum value of η_P (fig. 3), the blade-jet speed ratio is 0.61, the shift being caused by the decrease in the ratio η_P/η_W with increasing blade-jet speed ratio shown in figure 5.

The scatter in the data of figure 5, especially at a ratio of inlet total to outlet static pressure P_i/p_o of 5, is due to small
850 variations in the measured pressure ratio from the desired value. This pressure-ratio variation is evident in the following tabulation:

Inlet total pressure, P_i (in. Hg abs.)	Inlet total temperature, T_i ($^{\circ}$R)	Range of pressure ratio, P_i/p_o
20	1600	5.157 - 5.303
30	1200	4.965 - 5.122
30	1400	5.030 - 5.190
30	1600	4.977 - 5.212
30	1800	4.796 - 5.064

The relation between the ratio of inlet total to outlet static pressure P_i/p_o and the total-pressure ratio P_i/P_o is shown in figure 6 for all inlet total pressures and temperatures. Figure 7 shows the effect of the ratio of inlet total to outlet static pressure P_i/p_o on the turbine efficiency η_W at various blade-jet speed ratios for an inlet total pressure of 30 inches of mercury absolute and and inlet total temperature of 1400° R. As the pressure ratio increases from 1.5 to 5.0, the efficiency decreases 0.02 at a blade-jet speed ratio of 0.5. At lower blade-jet speed ratios, the efficiency is unaffected by pressure ratio. Figure 8 shows the effect of total-pressure ratio P_i/P_o on the turbine efficiency η_P for various blade-jet speed ratios. (The same data were used to cross-plot figs. 7 and 8.) The efficiency η_P increases a maximum of 0.07 at blade-jet speed ratios of 0.3 and 0.4 as the total-pressure ratio increases from 1.45 to 4.00. The efficiency increase is less at other blade-jet speed ratios. The difference in the trends of figures 7 and 8 is caused by the increase in the ratio η_P/η_W at low blade-jet speed ratios and high pressure ratios. (See fig. 5.)

The difference between the efficiencies η_W and η_P for any given data is due entirely to the difference in the corresponding value of the pressure ratios P_i/p_o and P_i/P_o. For any constant pressure ratio and blade-jet speed ratio, the ratio η_P/η_W is therefore constant for any inlet total pressure and temperature, and the efficiency trend with varying inlet total pressure and temperature is nearly the same for both η_P and η_W. Only the efficiency η_P is therefore shown as a function of inlet total pressure and inlet total temperature in figures 9 and 10, respectively.

The variation of the turbine efficiency η_P with inlet total pressure P_i for various blade-jet speed ratios is shown (fig. 9) for an inlet total temperature of 1600° R and a total-pressure ratio of 1.9. At a blade-jet speed ratio of 0.5, the efficiency increases 0.07 as the inlet total pressure increases from 20 to 50 inches of mercury absolute. The change in efficiency decreases with decreasing blade-jet speed ratio and is 0.04 at a blade-jet speed ratio of 0.2.

The turbine efficiency η_P decreases with increasing inlet total temperature at an inlet total pressure of 30 inches of mercury absolute and a total pressure ratio of 1.9 (fig. 10). The efficiency decreases 0.07 at a blade-jet speed ratio of 0.5 as the inlet total temperature increases from 1200° to 2160° R. As the blade-jet speed ratio decreases, the change in efficiency decreases and is 0.02 at a blade-jet speed ratio of 0.2.

The variation of turbine adiabatic efficiency with inlet total pressure and inlet total temperature may be a Reynolds number effect, as suggested in reference 3. In figure 11 the efficiency η_P is shown as a function of $P_i/T_i^{1.1}$, the Reynolds number factor derived in reference 3. The efficiency increases 0.09 at a blade-jet speed ratio of 0.5 as the Reynolds number factor increases from 0.006 to 0.015. The efficiency change over the same range of Reynolds number factors decreases with decreasing blade-jet speed ratio and is 0.03 at a blade-jet speed ratio of 0.2. At a total-pressure ratio P_i/P_o of 1.9, all data have good correlation. Similar plots at different pressure ratios show the same general trends. Part of this efficiency change may be caused by the heat lost to the cooling air.

The gas-flow factor $M_t\sqrt{\theta}/\delta$ is plotted as a function of corrected turbine speed $N/\sqrt{\theta}$ in figure 12. The data fall on lines of constant ratios of inlet total to outlet static pressure P_i/p_o. The data for pressure ratios of 4.0 and 5.0 fall on the same curve, which indicates that the critical pressure ratio occurs at or slightly below a pressure ratio of 4.0. The gas flow is restricted near the maximum attainable speed for pressure ratios less than critical and at low speeds for all pressure ratios. These restrictions may possibly be caused by such a change in the angle of the relative entering velocity that the effective flow area is decreased and the entering gas whirl is increased. Variation of gas-flow factor with turbine speed at pressure ratios above critical pressure ratio would seem to indicate that the critical pressure ratio occurs in the turbine wheel rather than in the nozzles.

Figure 13 is a cross plot of figure 12. For all speeds the critical pressure ratio is approximately 3.9. A convergent nozzle reaches critical flow at a pressure ratio slightly less than 1.9 for the gas conditions of this investigation. The resultant large pressure drop through the turbine wheel and the high value of blade-jet speed ratio at peak efficiency indicate a high degree of reaction, which is to be expected in a radial-flow turbine because the gas flows radially inward against centrifugal force.

SUMMARY OF RESULTS

From an efficiency investigation of the radial-flow turbine from a TT13-18 turbosupercharger over a turbine-speed range of 3000 to 24,000 rpm, an inlet-total-pressure range of 20 to 50 inches of mercury absolute, an inlet-total-temperature range of 1200° to 2160° R, and a total-pressure-ratio range of 1.45 to 4.0, the following results were obtained:

1. The maximum efficiency obtained based on total-pressure ratio and corrected for bearing friction η_P was 0.82 at an inlet total pressure of 50 inches of mercury absolute, an inlet total temperature of 1600° R, a total-pressure ratio of 1.46, and a blade-jet speed ratio of 0.62.

2. The following variations in efficiency with changes in inlet total pressure, inlet total temperature, total-pressure ratio, and blade-jet speed ratio occurred:

Change in turbine adiabatic efficiency η_P	Inlet total pressure P_1 (in. Hg abs.)	Inlet total temperature T_1 (°R)	Total-pressure ratio P_1/P_0	Blade-jet speed ratio U/V
0.07	30	1400	1.45 to 4.0	0.3 and 0.4
0.07 .04	20 to 50	1600	1.9	0.5 .2
-0.02 - .07	30	1200 to 2160	1.9	0.2 .5

3. When the effects of inlet total pressure and inlet total temperature on the turbine adiabatic efficiency were combined as an effect of a Reynolds number factor $P_1/T_1^{1.1}$, the efficiency η_P increased a maximum of 0.09 at a blade-jet speed ratio of 0.5 as the Reynolds number factor increased from 0.006 to 0.015.

4. The critical turbine pressure ratio, (inlet total to outlet static pressure) was approximately 3.9, which indicated that the turbine operates with considerable reaction.

Flight Propulsion Research Laboratory,
National Advisory Committee for Aeronautics,
Cleveland, Ohio.

Earl E. Coulter

Earl E. Coulter,
Mechanical Engineer.

W. R. Galloway

William R. Galloway,
Mechanical Engineer.

Approved:
Oscar W. Schey,
Mechanical Engineer.

jh

REFERENCES

1. Coulter, Earl E., Larkin, Robert G., and Gabriel, David S.: Efficiency of a Radial-Flow Exhaust-Gas Turbosupercharger Turbine with a 12.75-Inch Tip Diameter. NACA MR No. E6F03, 1945.

2. Pinkel, Benjamin, and Turner, L. Richard: Thermodynamic Data for the Computation of the Performance of Exhaust-Gas Turbines. NACA ARR No. 4B25, 1944.

3. Gabriel, David S., Carman, L. Robert, and Trautwein, Elmer E.: The Effect of Inlet Pressure and Temperature on the Efficiency of a Single-Stage Impulse Turbine Having an 11.0-Inch Pitch-Line Diameter Wheel. NACA ACR No. E5E19, 1945.

850

TABLE I - SUMMARY OF DATA FOR TURBINE OF TT13-18 TURBOSUPERCHARGER

Turbine speed, N (rpm)	Inlet total pressure, P_i (in. Hg abs.)	Pressure ratio		Blade-jet speed ratio, U/V	Turbine output (hp)	Gas weight flow, W_t (lb/sec)	Turbine adiabatic efficiencies		
		P_i/p_o	P_i/P_o				η_s	η_w	η_p
Inlet total temperature, T_i, 1200° R									
2,970	29.8	1.49	1.46	0.132	34.7	3.45	0.228	0.236	0.248
6,010	30.2	1.51	1.48	.265	67.0	3.55	.421	.437	.457
7,520	30.1	1.50	1.47	.332	79.5	3.56	.499	.520	.544
9,020	29.9	1.50	1.47	.399	89.6	3.53	.569	.595	.623
10,610	30.1	1.50	1.48	.468	99.3	3.53	.628	.662	.693
12,000	29.9	1.50	1.47	.530	106.2	3.50	.679	.720	.752
14,060	30.0	1.49	1.46	.627	105.2	3.48	.689	.744	.776
15,890	30.0	1.51	1.48	.701	110.3	3.46	.710	.777	.811
16,560	30.0	1.49	1.46	.738	104.4	3.45	.689	.763	.796
5,940	29.9	2.02	1.94	0.204	96.3	3.98	0.326	0.335	0.357
8,020	29.9	2.02	1.93	.276	125.6	4.01	.424	.436	.465
10,060	30.1	2.02	1.94	.344	149.3	4.04	.496	.513	.545
12,010	29.9	2.00	1.92	.415	168.3	4.05	.568	.590	.626
13,980	29.8	1.99	1.92	.485	188.3	4.01	.647	.675	.714
15,990	29.9	2.00	1.92	.552	204.2	4.01	.694	.730	.772
18,010	30.0	2.01	1.93	.619	209.9	4.03	.706	.750	.793
20,030	29.8	2.00	1.92	.692	198.3	4.00	.679	.733	.775
21,770	29.9	2.00	1.93	.752	192.7	3.96	.665	.729	.770
6,030	30.1	3.08	2.78	0.168	133.4	4.29	0.276	0.281	0.312
8,010	30.1	3.04	2.76	.224	170.6	4.27	.356	.364	.402
10,010	30.1	3.05	2.77	.279	207.2	4.29	.429	.439	.484
11,990	30.0	3.04	2.76	.335	235.9	4.30	.489	.502	.552
14,050	30.1	3.02	2.76	.393	267.5	4.31	.556	.574	.626
16,050	30.1	3.02	2.76	.449	299.0	4.29	.625	.647	.704
18,010	30.1	3.01	2.76	.505	313.7	4.29	.657	.684	.741
20,050	30.1	3.01	2.76	.562	317.9	4.29	.667	.700	.758
22,040	30.0	3.03	2.78	.616	320.7	4.25	.676	.717	.775
24,000	30.2	3.04	2.78	.670	320.9	4.29	.667	.713	.774
6,020	29.9	4.03	3.41	0.153	145.3	4.29	0.252	0.256	0.297
8,060	30.1	4.06	3.44	.205	188.6	4.33	.322	.328	.378
10,050	30.1	4.08	3.46	.255	230.4	4.34	.391	.399	.458
12,010	30.0	4.04	3.44	.306	263.9	4.35	.450	.461	.526
14,440	29.9	3.96	3.40	.368	306.7	4.34	.527	.542	.612
16,020	30.2	4.03	3.45	.408	335.6	4.36	.572	.589	.664
17,920	30.1	4.04	3.48	.456	358.3	4.34	.612	.634	.710
20,030	30.0	4.03	3.47	.510	366.1	4.33	.628	.655	.733
21,940	29.9	3.99	3.45	.559	373.0	4.31	.644	.677	.754
24,020	30.0	4.03	3.48	.612	388.5	4.33	.666	.705	.785
6,020	30.0	5.11	3.99	0.144	158.8	4.25	0.244	0.247	0.302
8,020	29.8	5.12	4.01	.191	205.1	4.26	.314	.319	.387
10,020	30.1	5.07	4.00	.240	249.7	4.31	.379	.386	.462
12,010	29.9	5.05	4.01	.287	286.8	4.31	.436	.446	.529
14,000	30.2	5.02	4.04	.335	328.2	4.29	.503	.516	.602
16,030	30.0	5.02	4.03	.384	371.7	4.31	.567	.583	.677
18,100	30.0	5.01	4.05	.434	399.8	4.31	.610	.630	.727
20,130	29.8	4.97	4.03	.484	410.5	4.30	.633	.657	.755
22,060	30.0	5.05	4.08	.528	418.0	4.31	.635	.664	.764
23,970	30.2	5.08	4.11	.573	432.3	4.33	.652	.686	.786

TABLE I - SUMMARY OF DATA FOR TURBINE OF TT13-18 TURBOSUPERCHARGER - Continued

Turbine speed, N (rpm)	Inlet total pressure, P_i (in. Hg abs.)	Pressure ratio		Blade-jet speed ratio, U/V	Turbine output (hp)	Gas weight flow, W_t (lb/sec)	Turbine adiabatic efficiencies		
		P_i/p_o	P_i/P_o				η_s	η_w	η_p
Inlet total temperature, T_i, 1400° R									
3,040	30.0	1.50	1.47	0.124	33.8	3.20	0.202	0.209	0.219
6,050	30.0	1.50	1.47	.247	62.6	3.25	.367	.382	.400
7,520	29.7	1.50	1.47	.307	76.9	3.23	.453	.472	.495
9,000	30.0	1.50	1.47	.369	86.8	3.26	.511	.536	.561
10,520	30.0	1.50	1.47	.431	97.1	3.28	.570	.600	.628
12,000	29.8	1.49	1.47	.493	101.6	3.21	.613	.652	.679
14,050	29.9	1.51	1.48	.572	110.9	3.25	.646	.695	.726
16,050	29.8	1.50	1.47	.655	106.8	3.22	.633	.696	.727
16,850	29.8	1.49	1.47	.691	103.0	3.16	.629	.699	.730
6,010	30.2	2.01	1.93	0.192	96.6	3.74	0.303	0.311	0.332
8,000	30.0	2.02	1.94	.256	126.1	3.72	.397	.408	.436
10,010	29.9	2.01	1.93	.320	146.8	3.75	.459	.474	.505
12,000	29.9	2.00	1.92	.384	168.1	3.75	.526	.546	.581
14,040	29.9	2.01	1.93	.449	190.4	3.74	.597	.623	.662
15,990	30.1	2.01	1.93	.511	206.2	3.76	.642	.675	.716
18,010	30.1	2.02	1.94	.576	212.2	3.75	.663	.704	.746
20,030	30.0	2.02	1.94	.640	209.2	3.73	.657	.707	.748
22,040	30.1	2.01	1.93	.705	204.2	3.73	.641	.701	.742
22,640	30.0	2.00	1.92	.724	204.0	3.70	.647	.710	.751
6,040	30.1	3.09	2.78	0.155	131.7	3.98	0.249	0.254	0.283
8,000	29.9	3.08	2.78	.206	169.6	3.97	.323	.330	.366
10,020	30.3	3.09	2.79	.257	208.3	4.02	.391	.400	.442
11,990	30.2	3.07	2.78	.308	235.9	3.99	.448	.460	.505
14,030	30.0	2.99	2.72	.365	261.3	3.97	.510	.526	.576
16,040	30.0	3.01	2.74	.416	294.2	4.00	.566	.587	.642
17,960	30.0	2.99	2.73	.467	312.2	3.96	.610	.636	.692
20,010	30.1	3.03	2.77	.518	323.7	3.99	.622	.652	.710
21,950	30.0	3.05	2.78	.566	327.8	3.96	.631	.667	.725
24,120	29.9	3.05	2.78	.622	342.5	3.96	.659	.702	.763
6,060	30.1	4.07	3.43	0.142	149.7	3.96	0.238	0.242	0.281
8,000	29.9	4.06	3.43	.187	194.0	3.97	.307	.313	.362
10,040	30.0	4.10	3.47	.235	237.2	3.96	.375	.383	.440
12,020	30.1	4.04	3.44	.282	275.3	4.01	.433	.443	.506
14,030	30.3	4.08	3.47	.328	314.7	4.05	.488	.501	.570
16,010	30.1	4.01	3.43	.377	346.1	4.04	.543	.560	.633
18,000	30.0	4.05	3.46	.422	375.0	4.03	.586	.606	.683
20,020	30.1	4.03	3.46	.470	382.4	4.04	.598	.622	.700
22,000	30.0	4.03	3.46	.516	396.1	4.02	.621	.651	.731
23,950	30.1	4.04	3.47	.562	412.4	4.03	.645	.680	.761
5,990	30.0	5.16	3.97	0.132	155.1	4.01	0.214	0.218	0.270
8,070	29.9	5.19	4.01	.177	205.6	4.00	.284	.289	.354
10,040	30.1	5.15	4.01	.221	248.3	4.01	.343	.350	.424
12,010	30.0	5.12	4.01	.264	290.2	4.02	.401	.410	.492
14,140	30.0	5.03	3.99	.313	335.0	4.03	.466	.478	.567
16,050	30.0	5.04	4.01	.355	368.6	4.03	.512	.527	.621
17,950	30.1	5.10	4.05	.396	402.1	4.05	.552	.570	.669
19,990	30.1	5.08	4.05	.441	417.0	4.03	.577	.599	.699
22,000	30.1	5.06	4.06	.486	432.7	4.03	.600	.626	.728
23,920	30.1	5.12	4.10	.526	455.4	4.03	.627	.658	.762

TABLE I - SUMMARY OF DATA FOR TURBINE OF TT13-18 TURBOSUPERCHARGER - Continued

Turbine speed, N (rpm)	Inlet total pressure, P_i (in. Hg abs.)	Pressure ratio P_i/p_o	Pressure ratio P_i/P_o	Blade-jet speed ratio, U/V	Turbine output (hp)	Gas weight flow, Wt (lb/sec)	Turbine adiabatic efficiencies η_s	η_W	η_P
Inlet total temperature, T_i, 1600° R									
3,030	20.1	1.52	1.49	0.114	23.9	2.05	0.188	0.198	0.208
5,990	20.2	1.53	1.50	.224	44.6	2.05	.347	.367	.385
7,510	20.0	1.53	1.50	.280	53.8	2.04	.420	.446	.467
9,000	20.0	1.53	1.50	.336	61.7	2.05	.479	.512	.536
10,520	20.1	1.52	1.50	.394	67.8	2.06	.529	.569	.595
12,020	20.1	1.52	1.49	.452	74.0	2.06	.580	.631	.661
12,980	20.1	1.52	1.50	.486	81.6	2.06	.636	.694	.724
14,050	20.1	1.52	1.49	.527	77.7	2.05	.610	.677	.706
14,750	20.1	1.52	1.50	.553	79.3	2.04	.624	.696	.727
13,000	20.1	1.53	1.50	.485	82.1	2.06	.636	.693	.724
3,990	20.2	2.07	1.98	0.116	46.0	2.30	0.194	0.201	0.215
6,030	20.2	2.04	1.96	.177	65.7	2.32	.279	.290	.310
7,970	20.1	2.05	1.96	.234	85.9	2.31	.366	.380	.405
9,990	20.1	2.05	1.97	.292	102.6	2.32	.434	.454	.483
12,020	20.0	2.03	1.95	.354	116.3	2.34	.494	.522	.555
14,050	20.1	2.02	1.94	.415	129.4	2.34	.552	.588	.624
16,020	20.1	2.04	1.96	.470	140.9	2.34	.594	.638	.677
18,000	20.1	2.04	1.96	.528	147.6	2.33	.625	.680	.720
19,630	20.1	2.04	1.96	.578	148.6	2.32	.635	.700	.741
5,980	20.2	3.11	2.80	0.143	87.2	2.45	0.233	0.240	0.266
8,030	20.1	3.09	2.79	.192	112.0	2.46	.300	.309	.343
10,000	20.1	3.09	2.79	.240	135.4	2.46	.363	.376	.416
11,980	20.1	3.07	2.78	.288	156.6	2.49	.416	.433	.478
13,990	20.1	3.06	2.78	.336	176.7	2.48	.473	.495	.544
16,000	20.1	3.08	2.79	.384	199.6	2.49	.529	.557	.611
18,020	20.1	3.07	2.78	.433	216.9	2.49	.577	.612	.668
20,010	20.1	3.09	2.81	.479	221.9	2.48	.589	.631	.688
22,060	20.2	3.10	2.82	.528	226.7	2.49	.598	.648	.706
23,630	20.2	3.07	2.80	.568	233.1	2.50	.618	.673	.733
6,000	20.1	4.05	3.43	0.131	95.4	2.45	0.213	0.219	0.254
8,010	20.1	4.12	3.46	.174	125.7	2.47	.277	.284	.330
10,000	20.2	4.08	3.45	.218	151.8	2.49	.333	.343	.395
12,010	20.2	4.05	3.43	.263	175.2	2.49	.386	.400	.459
13,950	20.2	4.08	3.46	.304	198.6	2.51	.432	.450	.514
16,050	20.2	4.07	3.47	.351	225.0	2.50	.492	.515	.584
18,030	20.2	4.08	3.48	.393	248.2	2.51	.540	.568	.643
20,030	20.2	4.08	3.49	.437	253.6	2.50	.554	.588	.663
22,050	20.1	4.07	3.49	.481	263.9	2.48	.581	.623	.699
24,050	20.2	4.06	3.49	.525	272.7	2.49	.599	.649	.726
6,030	20.2	5.28	4.06	0.123	105.4	2.47	0.203	0.208	0.257
8,030	20.2	5.30	4.07	.163	135.3	2.48	.259	.266	.327
10,000	20.1	5.16	4.02	.205	162.9	2.48	.316	.325	.394
12,000	20.1	5.17	4.03	.246	189.4	2.51	.363	.375	.453
14,080	20.1	5.16	4.04	.288	216.0	2.49	.417	.434	.519
16,020	20.1	5.27	4.11	.326	240.7	2.51	.456	.476	.568

TABLE I - SUMMARY OF DATA FOR TURBINE OF TT13-18 TURBOSUPERCHARGER - Continued

NACA

Turbine speed, N (rpm)	Inlet total pressure, P_i (in. Hg abs.)	Pressure ratio P_i/p_o	Pressure ratio P_i/P_o	Blade-jet speed ratio, U/V	Turbine output (hp)	Gas weight flow, W_t (lb/sec)	Turbine adiabatic efficiencies η_s	η_w	η_p
Inlet total temperature, T_i, 1600° R									
18,010	20.3	5.29	4.13	0.367	262.7	2.52	0.495	0.520	0.617
20,000	20.1	5.28	4.14	.407	274.1	2.51	.519	.549	.649
22,030	20.1	5.22	4.13	.450	286.6	2.51	.546	.582	.683
24,040	20.2	5.22	4.14	.491	296.8	2.51	.565	.608	.710
6,020	30.1	2.02	1.94	0.178	97.8	3.47	0.284	0.291	0.310
7,990	30.0	2.01	1.93	.238	124.8	3.47	.364	.375	.399
10,010	30.0	2.01	1.93	.297	150.9	3.50	.435	.449	.479
12,010	30.0	2.00	1.92	.357	171.2	3.51	.494	.513	.545
13,980	30.0	2.00	1.92	.416	194.8	3.53	.559	.583	.620
16,030	30.0	2.01	1.93	.476	213.2	3.53	.610	.641	.680
18,030	30.0	2.01	1.93	.535	226.1	3.51	.650	.688	.729
20,020	30.0	2.02	1.94	.593	224.5	3.48	.649	.695	.737
22,070	30.0	2.00	1.92	.658	218.8	3.47	.642	.698	.738
22,900	30.1	1.99	1.91	.685	216.1	3.47	.639	.699	.741
6,050	30.2	3.01	2.73	0.146	132.6	3.67	0.243	0.247	0.275
8,000	29.8	2.97	2.70	.195	169.2	3.68	.313	.319	.353
10,000	30.0	2.97	2.70	.243	203.3	3.71	.372	.381	.420
12,030	30.0	2.97	2.70	.293	234.3	3.72	.428	.440	.483
13,990	30.1	2.99	2.72	.340	269.4	3.73	.489	.504	.552
16,040	29.9	2.99	2.72	.390	301.2	3.71	.549	.568	.622
18,040	30.0	3.01	2.75	.436	325.7	3.73	.586	.609	.664
20,040	30.0	3.00	2.74	.487	334.5	3.72	.608	.636	.694
22,010	30.0	3.03	2.77	.532	346.4	3.73	.620	.654	.713
23,970	29.9	3.06	2.79	.576	358.3	3.72	.638	.678	.739
6,020	50.2	1.49	1.47	0.231	116.5	5.12	0.385	0.393	0.413
8,020	50.0	1.49	1.47	.308	150.5	5.08	.501	.513	.537
10,020	50.1	1.49	1.46	.385	173.0	5.15	.569	.585	.613
11,990	49.9	1.49	1.47	.461	202.8	5.08	.675	.696	.728
14,120	50.0	1.49	1.47	.542	219.2	5.07	.730	.759	.793
16,030	49.9	1.49	1.46	.619	222.5	5.05	.752	.788	.823
18,110	50.0	1.48	1.46	.701	208.5	5.06	.707	.751	.785
20,040	49.8	1.47	1.45	.782	185.2	4.95	.653	.709	.741
6,120	50.0	2.00	1.92	0.183	181.9	5.76	0.323	0.327	0.348
8,060	50.0	1.97	1.90	.242	226.0	5.76	.407	.413	.439
10,010	50.1	1.97	1.90	.301	268.8	5.84	.477	.485	.516
12,020	49.9	1.97	1.89	.362	313.2	5.83	.557	.569	.604
14,020	50.3	2.00	1.92	.419	356.0	5.89	.618	.632	.671
16,020	50.1	1.99	1.92	.478	386.1	5.83	.677	.695	.737
18,060	50.2	2.00	1.92	.539	413.9	5.81	.727	.750	.793
20,000	50.0	2.00	1.93	.595	411.6	5.78	.722	.749	.792
22,130	50.3	1.99	1.92	.661	405.2	5.81	.713	.747	.789
23,950	50.3	1.99	1.91	.716	402.7	5.80	.711	.750	.793
6,010	50.0	2.95	2.68	0.147	234.7	6.10	0.263	0.265	0.294
8,020	50.2	2.94	2.68	.196	303.9	6.17	.337	.341	.375
10,030	50.3	2.91	2.66	.247	368.8	6.20	.412	.418	.458
11,990	50.2	2.91	2.66	.294	429.1	6.19	.478	.485	.531
14,030	50.2	2.93	2.68	.343	487.3	6.19	.539	.548	.598
16,060	50.4	2.93	2.68	.393	546.5	6.20	.604	.616	.670
18,070	50.2	2.96	2.71	.440	597.2	6.21	.654	.669	.727
20,080	50.0	2.96	2.71	.490	622.0	6.17	.687	.704	.764
22,070	50.2	3.01	2.75	.534	652.6	6.20	.707	.728	.791
24,020	50.4	3.00	2.75	.582	670.6	6.20	.727	.752	.825

TABLE I - SUMMARY OF DATA FOR TURBINE OF TT13-18 TURBOSUPERCHARGER - Continued

NACA

Turbine speed, N (rpm)	Inlet total pressure, P_i (in. Hg abs.)	Pressure ratio P_i/p_o	Pressure ratio P_i/P_o	Blade-jet speed ratio, U/V	Turbine output (hp)	Gas weight flow, W_t (lb/sec)	Turbine adiabatic efficiencies η_s	η_w	η_p
Inlet total temperature, T_i, 1800° R									
6,010	30.0	2.01	1.92	0.168	96.7	3.27	0.266	0.273	0.291
8,130	29.9	2.00	1.91	.228	124.1	3.27	.343	.353	.376
10,020	29.9	2.02	1.92	.280	151.1	3.29	.410	.423	.452
11,990	30.1	2.02	1.93	.334	173.2	3.32	.464	.482	.513
14,050	30.0	2.01	1.92	.393	195.3	3.33	.527	.550	.586
16,030	30.2	2.02	1.94	.447	216.3	3.35	.574	.602	.639
17,980	30.0	2.02	1.93	.501	227.2	3.32	.610	.645	.686
20,080	30.1	1.99	1.90	.566	230.8	3.32	.632	.675	.717
22,000	30.0	2.02	1.93	.613	231.3	3.29	.626	.678	.718
23,660	30.1	2.02	1.93	.660	226.3	3.30	.611	.670	.712
Inlet total temperature, T_i, 2000° R									
3,050	30.1	1.51	1.48	0.104	35.1	2.71	0.171	0.177	0.185
6,000	30.0	1.51	1.48	.204	65.1	2.74	.313	.325	.341
7,520	30.0	1.51	1.48	.255	80.2	2.75	.384	.400	.420
9,020	30.1	1.51	1.48	.306	93.3	2.74	.449	.469	.493
10,560	30.0	1.50	1.48	.358	104.9	2.76	.501	.526	.552
12,020	30.0	1.50	1.48	.408	114.1	2.75	.547	.578	.605
13,910	30.0	1.50	1.47	.473	122.0	2.75	.588	.628	.658
15,900	30.0	1.51	1.48	.539	135.0	2.75	.647	.697	.730
17,260	30.0	1.50	1.48	.587	134.6	2.74	.651	.709	.740
18,720	30.1	1.50	1.47	.638	133.0	2.74	.646	.713	.746
6,040	30.0	2.02	1.93	0.160	101.8	3.11	0.262	0.268	0.280
8,010	30.1	2.01	1.93	.212	128.4	3.12	.330	.339	.362
10,000	30.0	2.01	1.92	.265	155.9	3.12	.401	.413	.427
12,020	30.0	2.00	1.92	.319	176.1	3.13	.454	.470	.483
14,180	30.0	2.01	1.93	.375	204.2	3.14	.521	.543	.555
15,980	29.9	1.99	1.91	.426	228.1	3.14	.590	.618	.628
18,010	30.1	2.00	1.92	.480	245.8	3.15	.634	.668	.674
20,030	30.1	2.01	2.93	.530	250.0	3.14	.638	.679	.676
22,050	30.0	2.02	1.95	.581	246.8	3.11	.631	.679	.667
23,980	30.0	2.01	1.94	.635	237.5	3.10	.614	.672	.649
5,950	30.1	3.13	2.81	0.126	133.4	3.29	0.210	0.213	0.238
8,020	30.1	3.08	2.78	.171	174.5	3.30	.277	.282	.314
10,030	30.0	3.05	2.75	.215	210.3	3.32	.335	.342	.379
12,000	30.1	3.04	2.75	.258	248.6	3.32	.395	.405	.448
13,990	30.1	3.04	2.76	.300	280.6	3.34	.444	.457	.504
16,000	29.9	3.04	2.76	.344	315.4	3.31	.504	.521	.572
18,000	30.0	3.06	2.78	.385	344.6	3.34	.541	.561	.617
20,000	30.1	3.02	2.75	.431	354.6	3.34	.563	.589	.645
22,030	30.0	3.02	2.75	.474	371.2	3.32	.594	.624	.682
23,970	30.1	3.04	2.76	.515	386.6	3.34	.612	.647	.708
5,980	30.6	4.14	3.48	0.116	146.1	3.33	0.188	0.191	0.224
8,030	30.1	4.07	3.42	.156	189.1	3.35	.244	.249	.290
10,010	30.1	4.03	3.40	.195	231.3	3.35	.300	.306	.355
11,970	30.1	4.04	3.41	.233	274.3	3.36	.355	.363	.419
14,170	30.0	3.95	3.36	.278	317.6	3.35	.417	.429	.490
15,990	30.0	4.05	3.43	.312	353.9	3.35	.459	.473	.540
17,990	30.2	4.05	3.44	.351	386.9	3.36	.500	.517	.588
19,950	30.1	4.03	3.43	.389	400.8	3.36	.519	.539	.612
22,010	30.1	4.01	3.44	.430	428.3	3.35	.559	.583	.658
23,870	29.9	4.03	3.45	.465	451.0	3.34	.587	.616	.695

TABLE I - SUMMARY OF DATA FOR TURBINE OF TT13-18 TURBOSUPERCHARGER - Concluded

Turbine speed, N (rpm)	Inlet total pressure, P_i (in. Hg abs.)	Pressure ratio P_i/p_o	Pressure ratio P_i/P_o	Blade-jet speed ratio, U/V	Turbine output (hp)	Gas weight flow, W_t (lb/sec)	Turbine adiabatic efficiencies η_s	η_w	η_p
Inlet total temperature, T_i, 2160° R									
3,010	30.0	1.51	1.48	0.098	34.7	2.60	0.162	0.168	0.176
6,010	29.9	1.51	1.48	.195	65.6	2.62	.304	.315	.331
7,540	30.0	1.50	1.47	.247	80.4	2.66	.372	.387	.406
9,010	30.0	1.51	1.48	.293	92.9	2.64	.428	.448	.469
10,520	30.1	1.50	1.47	.344	103.2	2.68	.471	.495	.520
11,970	30.1	1.50	1.47	.392	112.5	2.68	.516	.545	.572
13,920	29.9	1.50	1.47	.458	121.7	2.65	.569	.608	.637
15,800	30.0	1.50	1.48	.515	132.6	2.68	.604	.650	.681
17,030	29.9	1.51	1.48	.555	133.3	2.64	.615	.670	.700
18,030	30.0	1.50	1.47	.591	132.1	2.64	.617	.678	.710
18,450	30.0	1.50	1.47	.604	132.3	2.65	.613	.676	.708
6,070	30.1	2.02	1.93	0.154	98.2	3.00	0.241	0.247	0.263
7,990	30.1	2.01	1.93	.202	126.3	3.01	.308	.317	.338
10,040	30.0	2.01	1.93	.254	152.5	3.02	.371	.383	.408
11,980	30.1	2.02	1.93	.303	174.1	3.04	.418	.434	.463
13,980	30.0	2.02	1.94	.353	195.8	3.05	.469	.489	.521
16,060	30.0	2.02	1.94	.406	223.4	3.05	.536	.561	.596
18,040	30.0	2.02	1.94	.455	242.0	3.06	.575	.606	.644
19,990	30.1	2.01	1.93	.508	240.7	3.05	.582	.621	.660
22,080	30.0	2.01	1.93	.561	240.5	3.02	.588	.635	.673
6,050	30.3	3.08	2.77	0.124	129.5	3.18	0.196	0.200	0.223
8,030	30.0	3.02	2.73	.166	168.2	3.18	.259	.264	.294
10,020	30.2	2.99	2.71	.208	203.0	3.20	.313	.321	.355
11,990	30.0	2.98	2.70	.249	235.4	3.19	.364	.374	.413
13,960	30.0	3.00	2.72	.289	268.0	3.21	.410	.422	.466
16,000	30.0	3.01	2.73	.331	306.2	3.21	.467	.483	.531
17,950	30.0	3.02	2.74	.371	334.6	3.22	.508	.528	.580
20,010	30.1	3.02	2.74	.413	351.8	3.24	.531	.555	.609
22,080	30.2	3.02	2.75	.456	366.2	3.23	.554	.583	.638
23,980	30.0	3.01	2.74	.496	376.1	3.22	.572	.606	.664
20,170	30.1	3.02	2.74	.417	356.5	3.23	.540	.564	.619

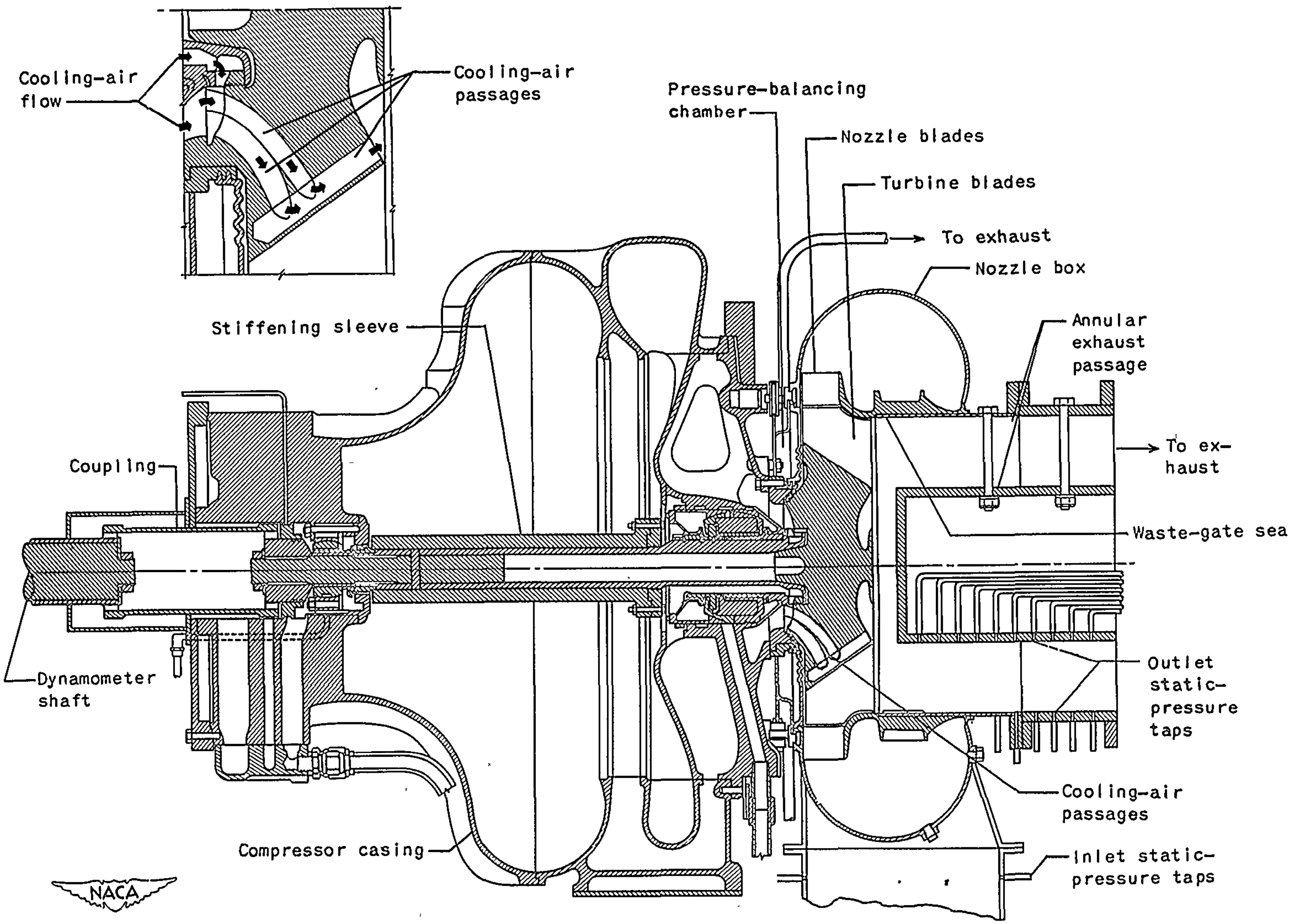

Figure 1. - Setup for investigation of turbine from Turbo Engineering Corporation TT13-18 turbosupercharger.

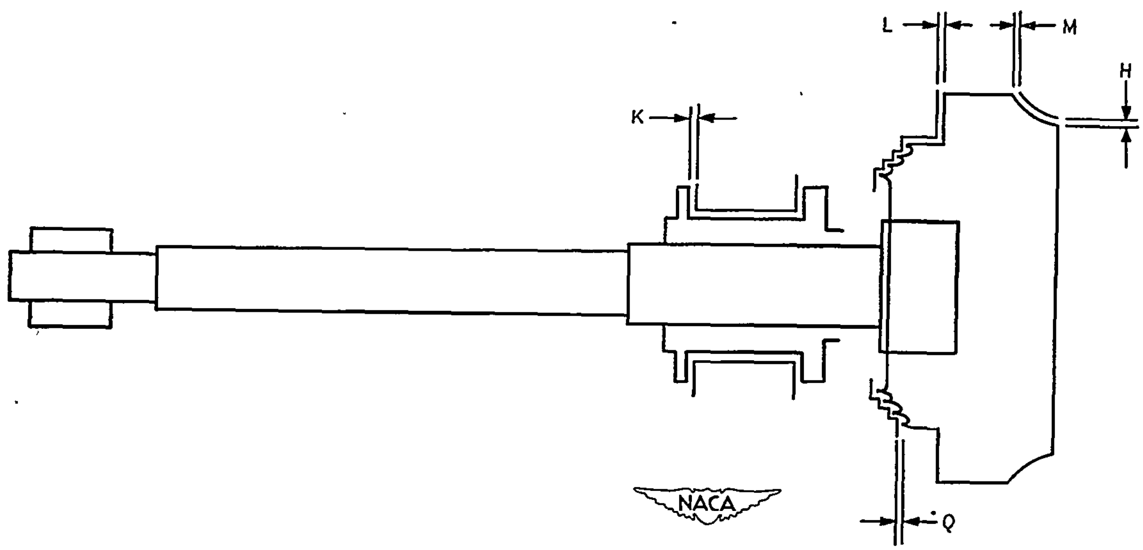

		Cold clearances before running (in.)	Cold clearances after 86 operating hours (in.)
H	Trailing edge (radial)		
	Top	0.040	0.044
	Right-hand side	.043	.041
	Bottom	.043	.028
	Left-hand side	.041	.030
K	Thrust bearing	.002	.002
L	Blade front	.048	.032
M	Blade rear	.052	.033
Q	Cooling-air seal	.004	.009

Figure 2. - Diagram of turbine clearances.

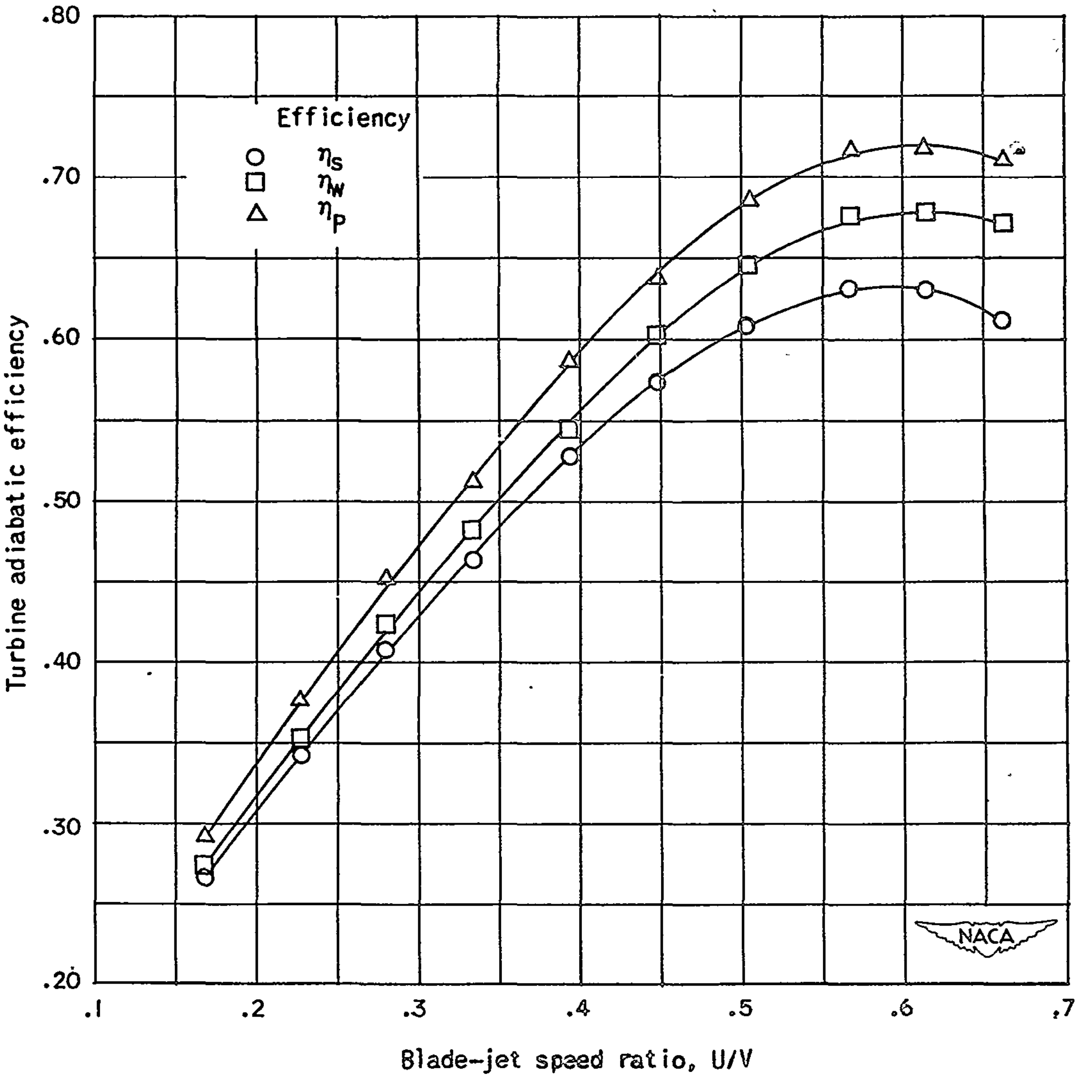

Figure 3. - Comparison of turbine adiabatic efficiencies η_s, η_W, η_P: Inlet total pressure P_i, 30 inches mercury absolute; inlet total temperature T_i, 1800° R; pressure ratios P_i/p_o, 2.0; P_i/P_o, 1.9.

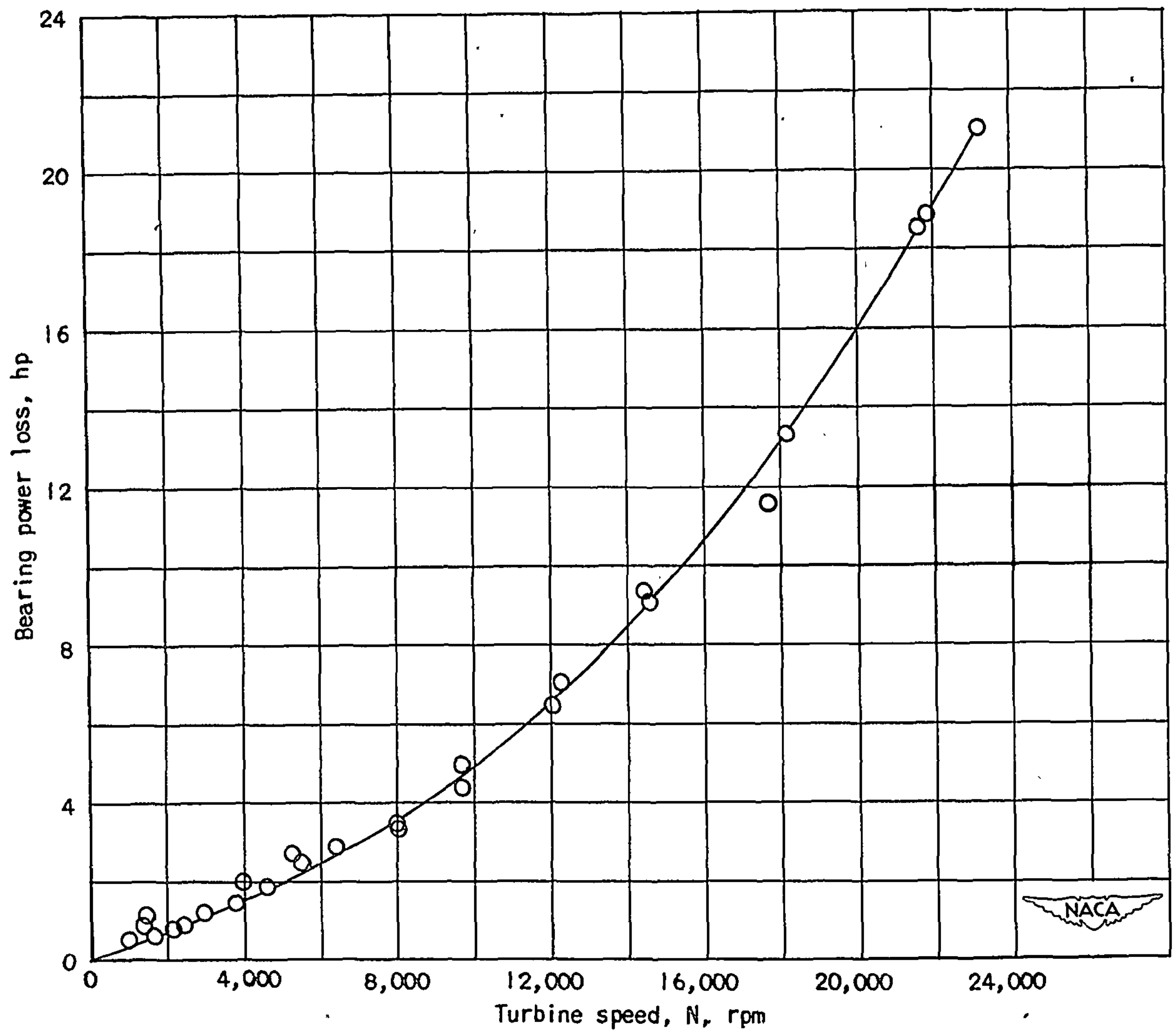

Figure 4. - Variation of bearing power loss with turbine speed.

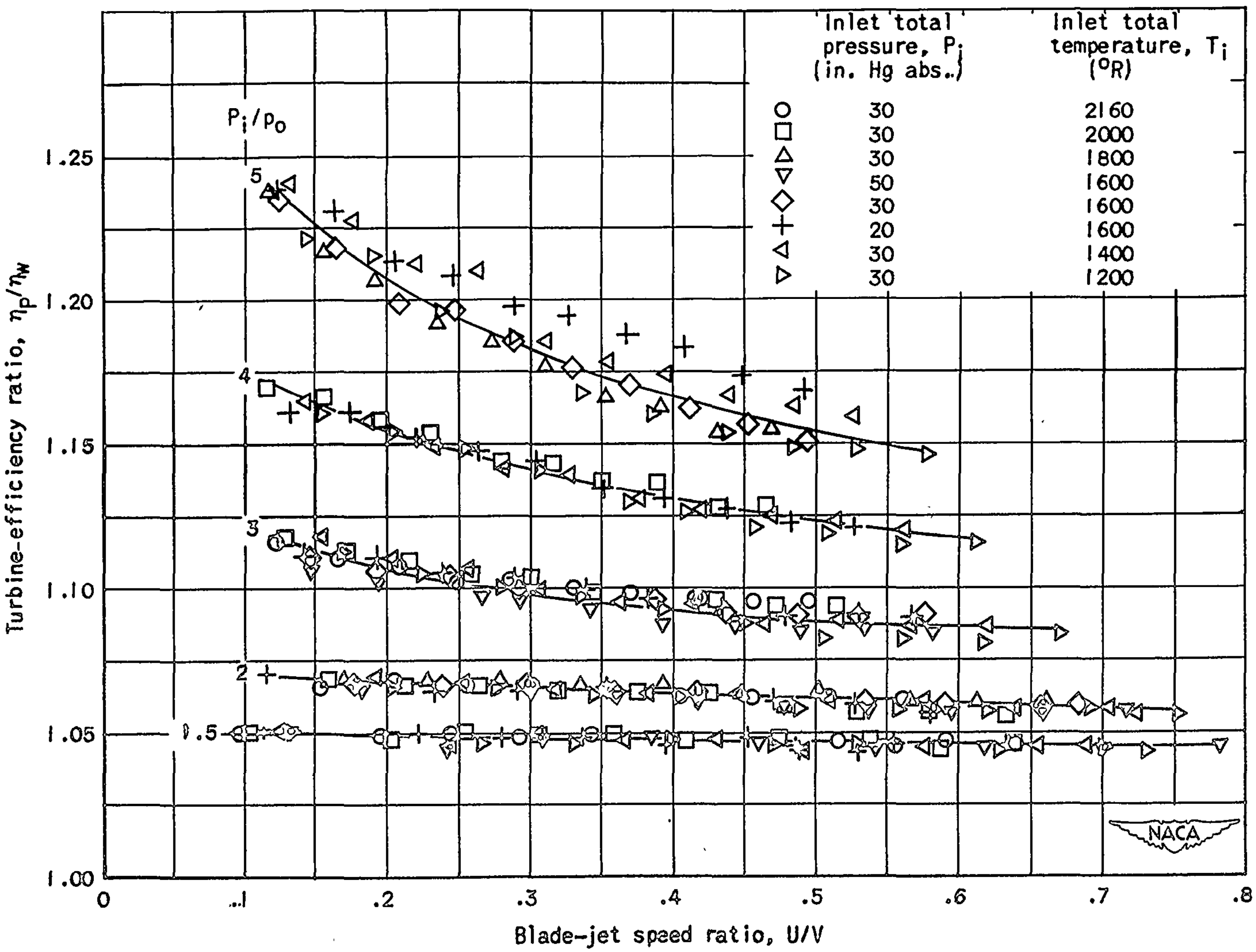

Figure 5. - Variation of turbine-efficiency ratio with blade-jet speed ratio for various pressure ratios.

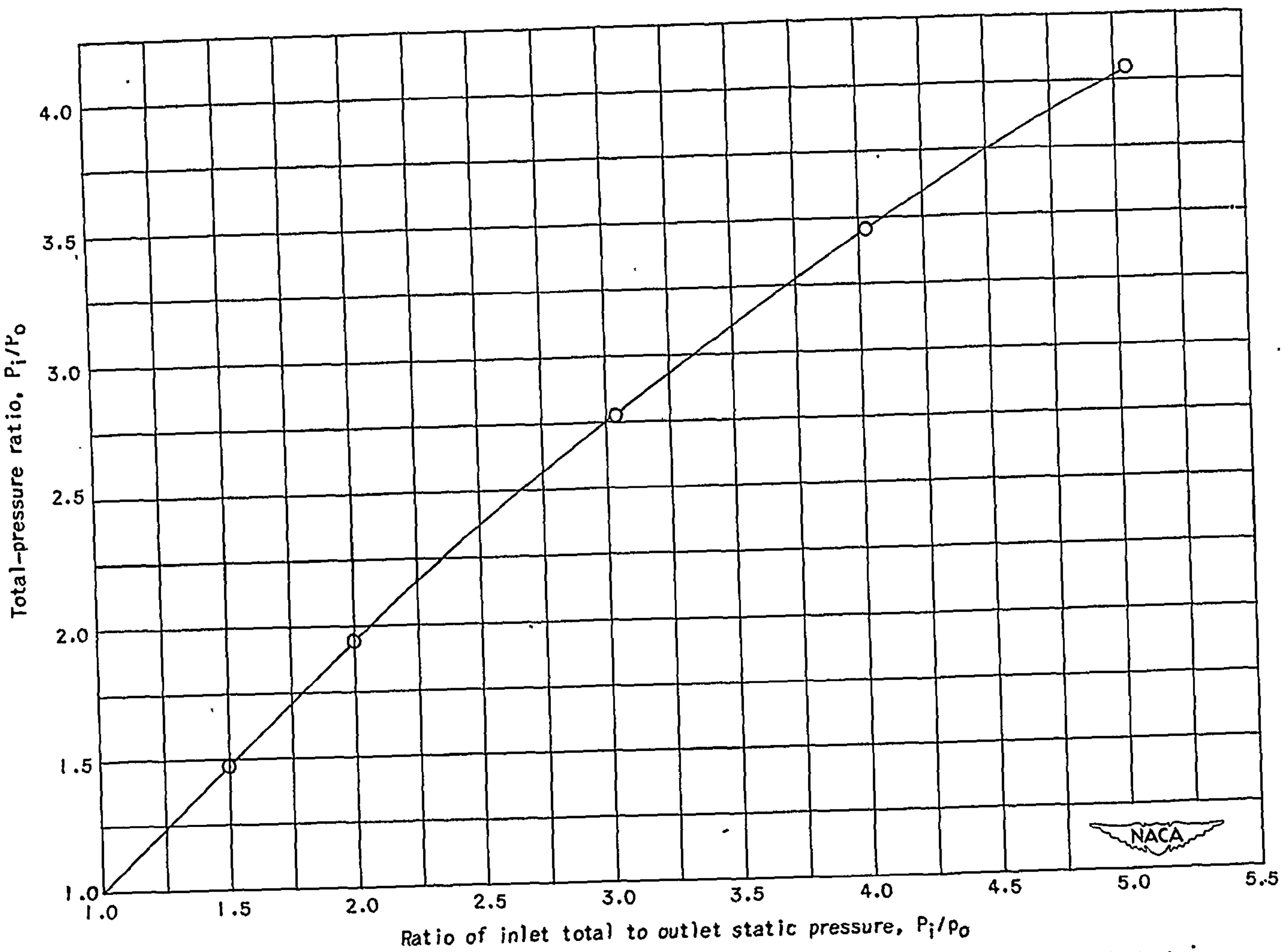

Figure 6. - Relation between ratio of inlet total to outlet static pressure and total-pressure ratio.

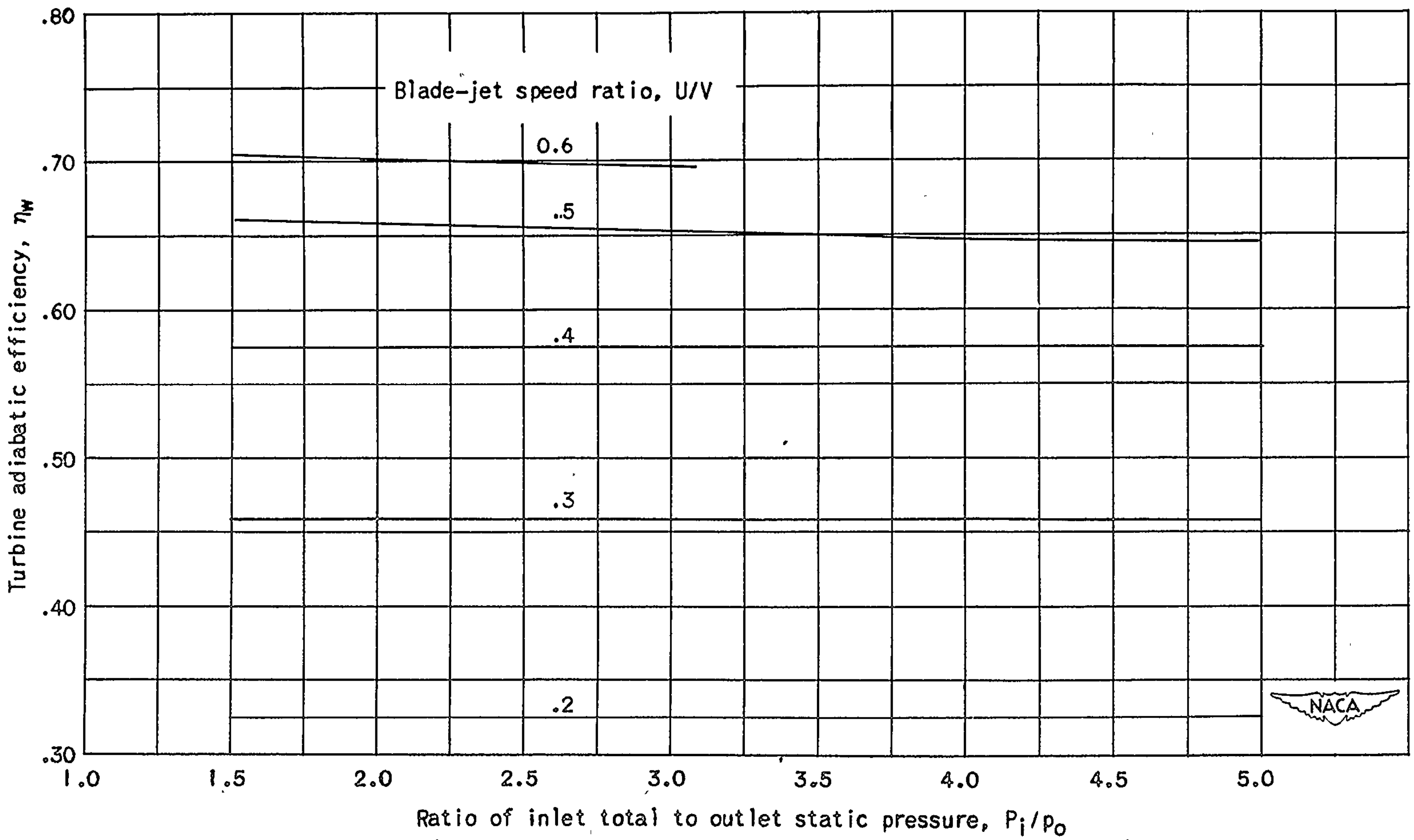

Figure 7. - Effect of ratio of inlet total to outlet static pressure on turbine adiabatic efficiency η_w. Inlet total pressure P_i, 30 inches mercury absolute; inlet total temperature T_i, 1400° R.

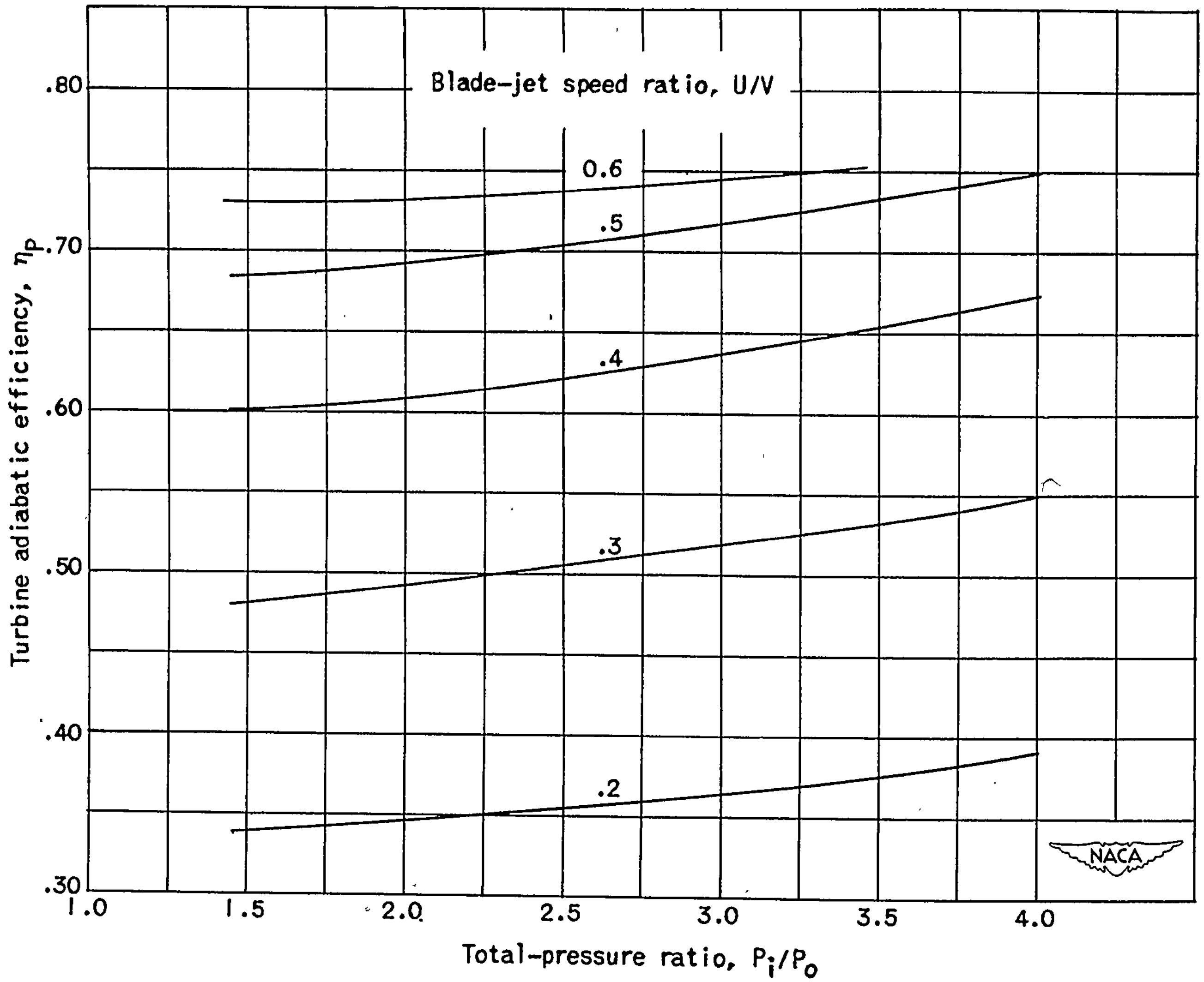

Figure 8. – Effect of total-pressure ratio on turbine adiabatic efficiency η_p. Inlet total pressure P_i, 30 inches mercury absolute; inlet total temperature T_i, 1400° R.

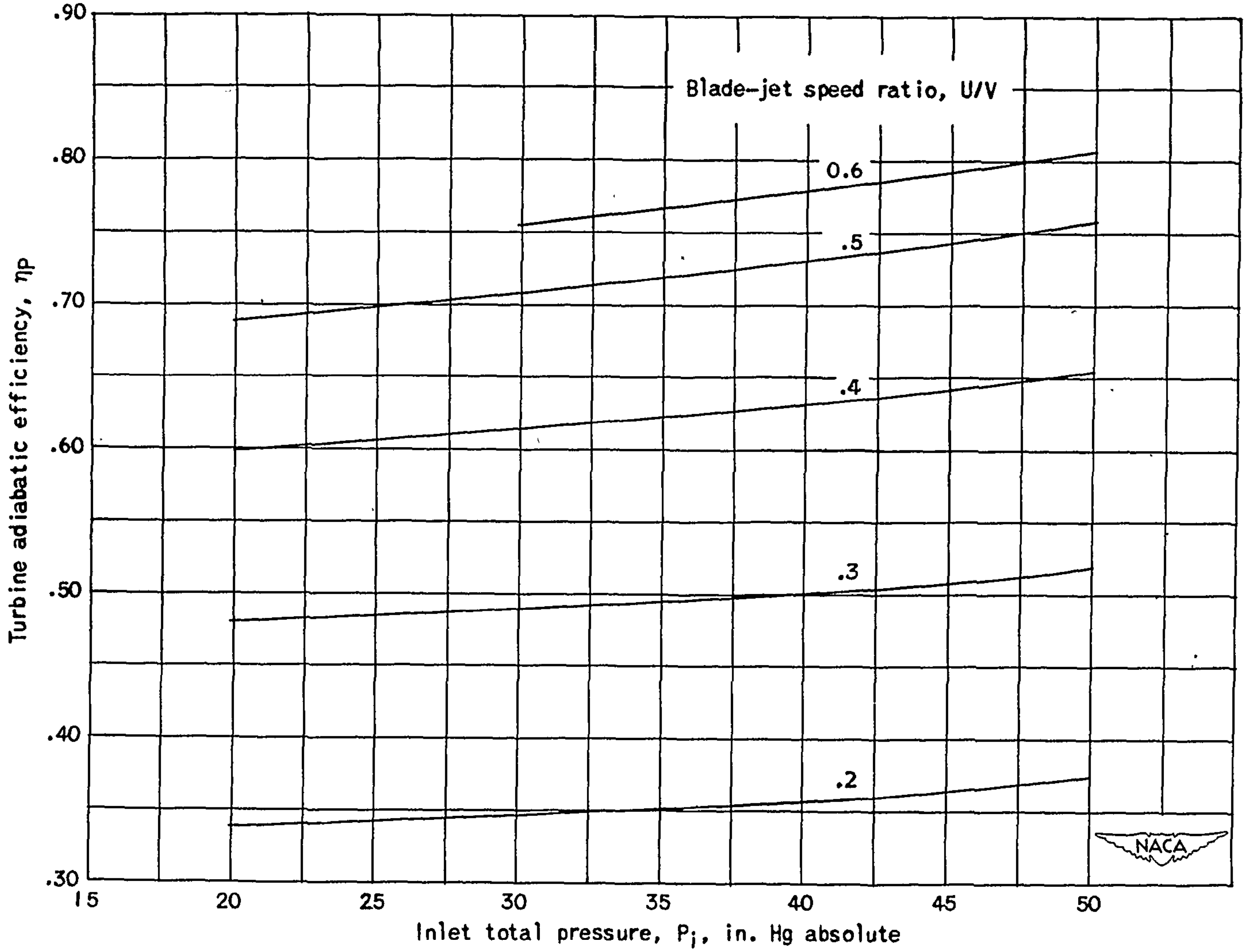

Figure 9. - Effect of inlet total pressure on turbine adiabatic efficiency η_P. Inlet total temperature T_i, 1600° R; total-pressure ratio P_i/P_o, 1.9.

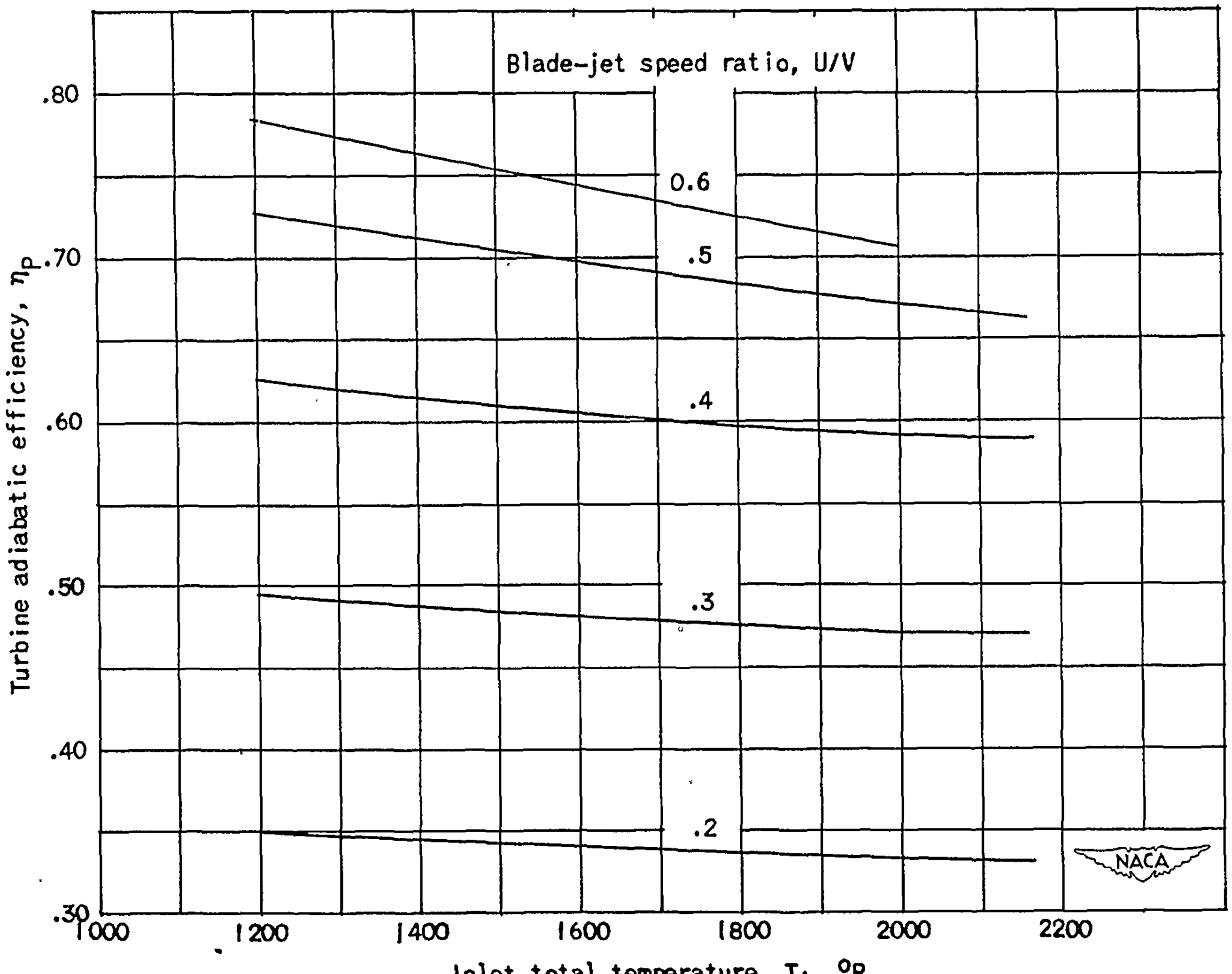

Figure 10. - Effect of inlet total temperature on turbine adiabatic efficiency η_p. Inlet total pressure P_i, 30 inches mercury absolute; total-pressure ratio P_i/P_o, 1.9.

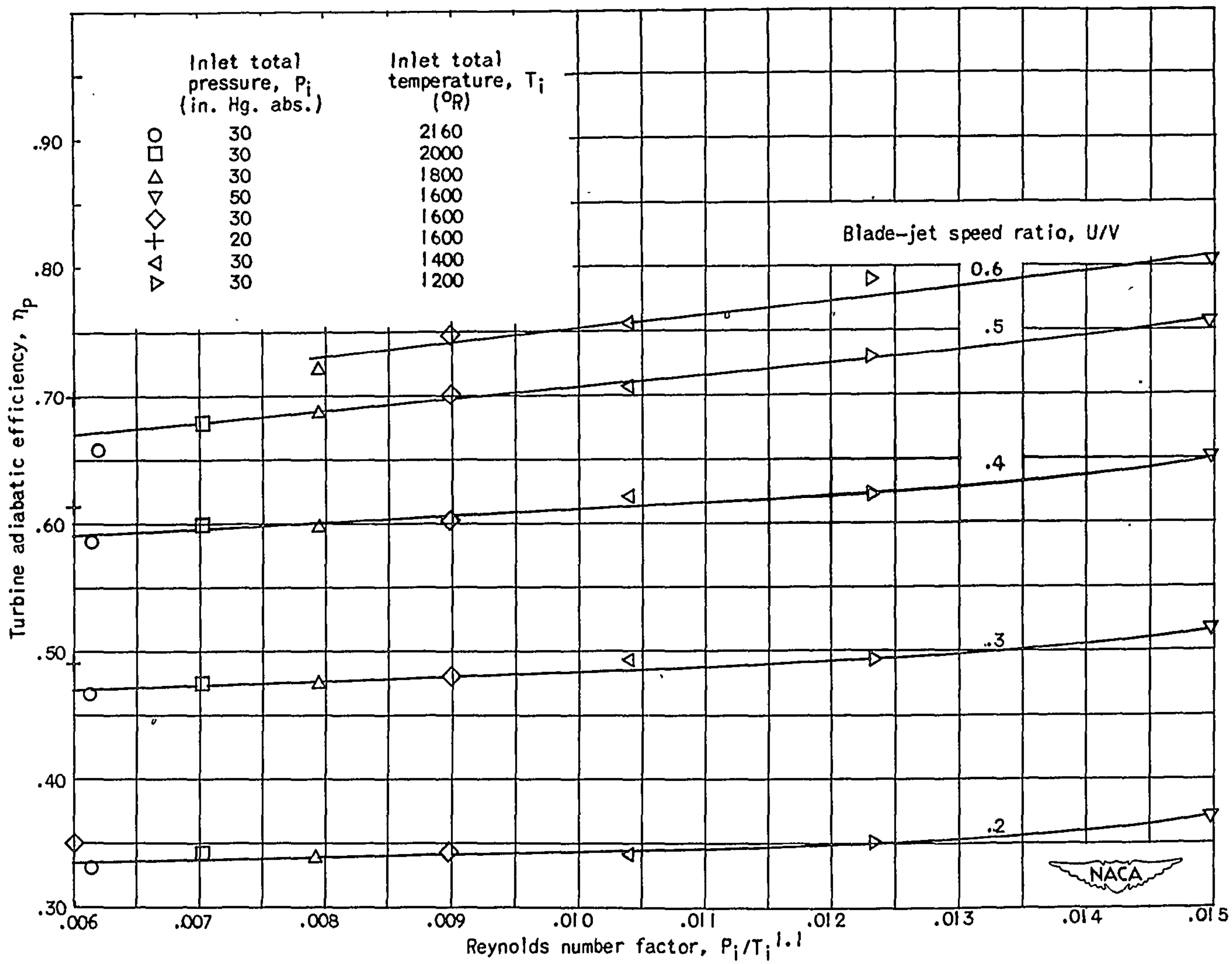

Figure 11. - Effect of Reynolds number factor on turbine adiabatic efficiency η_p at total-pressure ratio P_i/P_o of 1.9.

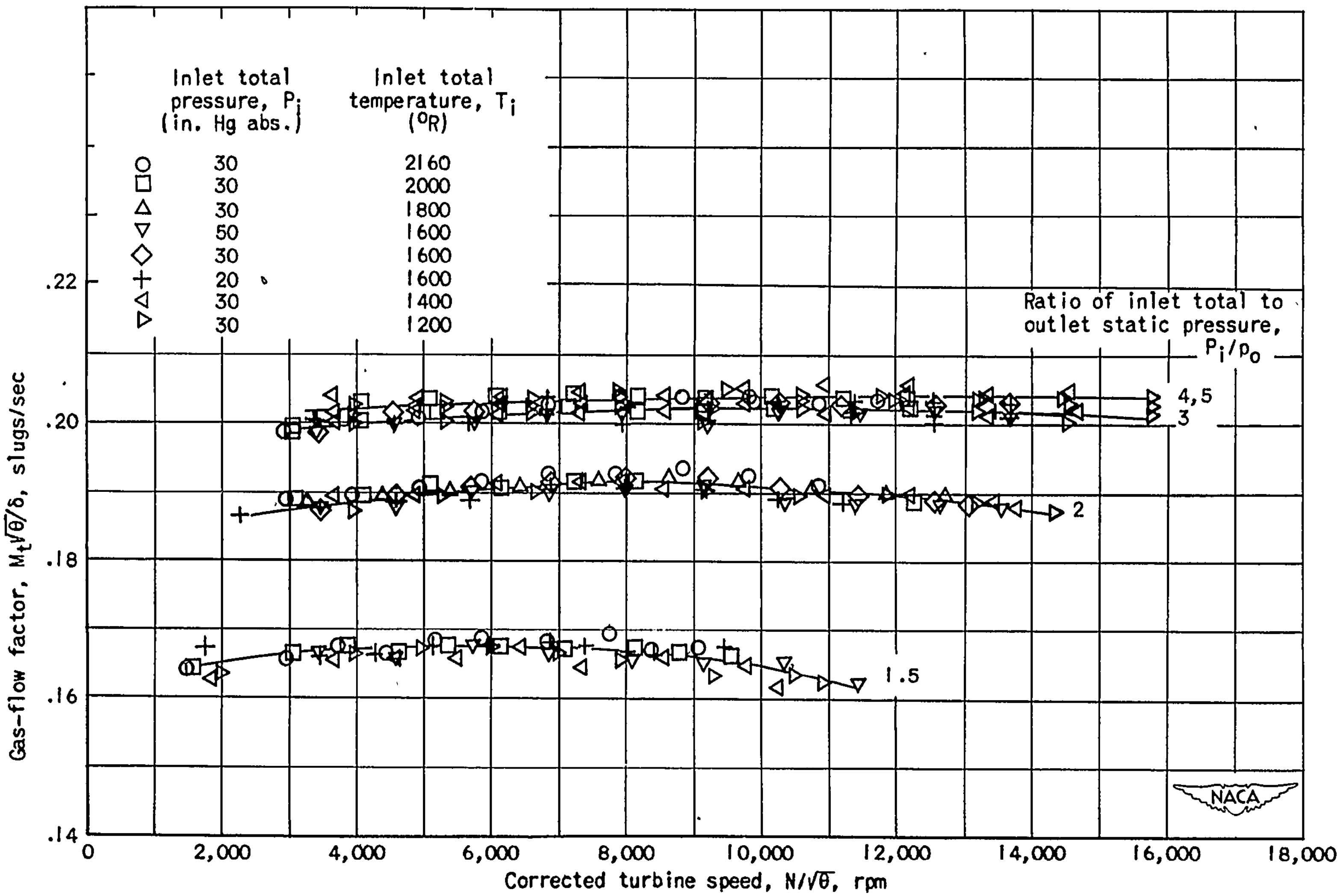

Figure 12. - Variation of gas-flow factor with corrected turbine speed over a range of pressure ratios.

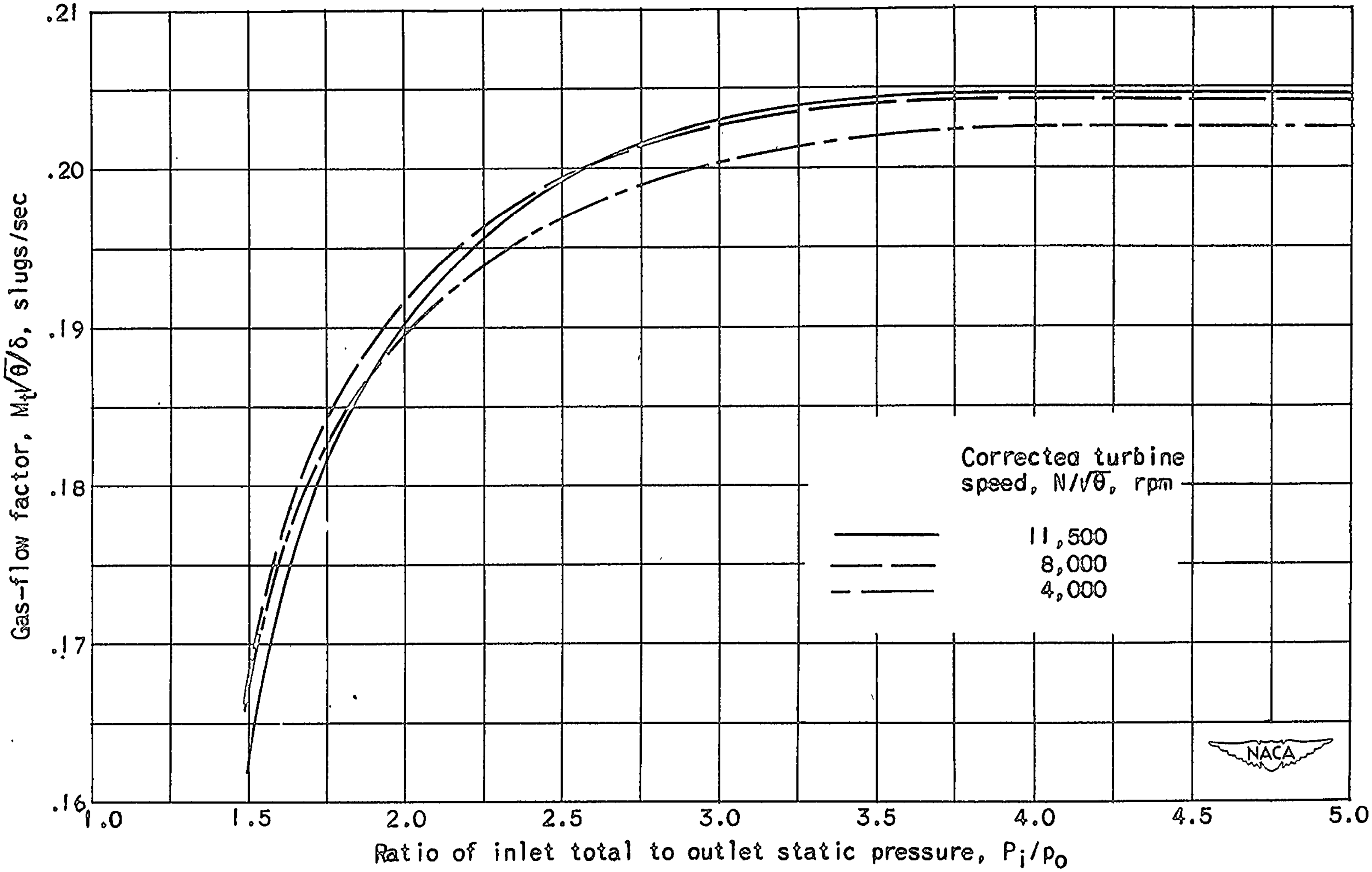

Figure 13. - Variation of gas-flow factor with pressure ratio over a range of speeds. (Cross plot of fig. 12.)